



University of
Massachusetts
Amherst

Measurement of $B \rightarrow X$ gamma Decays and Determination of $|V_{td}/V_{ts}|$

Item Type	article
DOI	10.1103/PhysRevLett.102.161803
Download date	2024-12-04 09:19:15
Link to Item	https://hdl.handle.net/20.500.14394/5976

Measurement of $B \rightarrow X\gamma$ Decays and Determination of $|V_{td}/V_{ts}|$

B. Aubert,¹ M. Bona,¹ Y. Karyotakis,¹ J. P. Lees,¹ V. Poireau,¹ E. Prencipe,¹ X. Prudent,¹ V. Tisserand,¹ J. Garra Tico,² E. Grauges,² L. Lopez,^{3a,3b} A. Palano,^{3a,3b} M. Pappagallo,^{3a,3b} G. Eigen,⁴ B. Stugu,⁴ L. Sun,⁴ G. S. Abrams,⁵ M. Battaglia,⁵ D. N. Brown,⁵ R. N. Cahn,⁵ R. G. Jacobsen,⁵ L. T. Kerth,⁵ Yu. G. Kolomensky,⁵ G. Lynch,⁵ I. L. Osipenko,⁵ M. T. Ronan,^{5,*} K. Tackmann,⁵ T. Tanabe,⁵ C. M. Hawkes,⁶ N. Soni,⁶ A. T. Watson,⁶ H. Koch,⁷ T. Schroeder,⁷ D. Walker,⁸ D. J. Asgeirsson,⁹ B. G. Fulsom,⁹ C. Hearty,⁹ T. S. Mattison,⁹ J. A. McKenna,⁹ M. Barrett,¹⁰ A. Khan,¹⁰ V. E. Blinov,¹¹ A. D. Bukin,¹¹ A. R. Buzykaev,¹¹ V. P. Druzhinin,¹¹ V. B. Golubev,¹¹ A. P. Onuchin,¹¹ S. I. Serednyakov,¹¹ Yu. I. Skovpen,¹¹ E. P. Solodov,¹¹ K. Yu. Todyshev,¹¹ M. Bondioli,¹² S. Curry,¹² I. Eschrich,¹² D. Kirkby,¹² A. J. Lankford,¹² P. Lund,¹² M. Mandelkern,¹² E. C. Martin,¹² D. P. Stoker,¹² S. Abachi,¹³ C. Buchanan,¹³ J. W. Gary,¹⁴ F. Liu,¹⁴ O. Long,¹⁴ B. C. Shen,^{14,*} G. M. Vitug,¹⁴ Z. Yasin,¹⁴ L. Zhang,¹⁴ V. Sharma,¹⁵ C. Campagnari,¹⁶ T. M. Hong,¹⁶ D. Kovalskiy,¹⁶ M. A. Mazur,¹⁶ J. D. Richman,¹⁶ T. W. Beck,¹⁷ A. M. Eisner,¹⁷ C. J. Flacco,¹⁷ C. A. Heusch,¹⁷ J. Kroseberg,¹⁷ W. S. Lockman,¹⁷ A. J. Martinez,¹⁷ T. Schalk,¹⁷ B. A. Schumm,¹⁷ A. Seiden,¹⁷ M. G. Wilson,¹⁷ L. O. Winstrom,¹⁷ C. H. Cheng,¹⁸ D. A. Doll,¹⁸ B. Echenard,¹⁸ F. Fang,¹⁸ D. G. Hitlin,¹⁸ I. Narsky,¹⁸ T. Piatenko,¹⁸ F. C. Porter,¹⁸ R. Andreassen,¹⁹ G. Mancinelli,¹⁹ B. T. Meadows,¹⁹ K. Mishra,¹⁹ M. D. Sokoloff,¹⁹ P. C. Bloom,²⁰ W. T. Ford,²⁰ A. Gaz,²⁰ J. F. Hirschauer,²⁰ M. Nagel,²⁰ U. Nauenberg,²⁰ J. G. Smith,²⁰ K. A. Ulmer,²⁰ S. R. Wagner,²⁰ R. Ayad,^{21,†} A. Soffer,^{21,‡} W. H. Toki,²¹ R. J. Wilson,²¹ D. D. Altenburg,²² E. Feltresi,²² A. Hauke,²² H. Jasper,²² M. Karbach,²² J. Merkel,²² A. Petzold,²² B. Spaan,²² K. Wacker,²² M. J. Kobel,²³ W. F. Mader,²³ R. Nogowski,²³ K. R. Schubert,²³ R. Schwierz,²³ A. Volk,²³ D. Bernard,²⁴ G. R. Bonneaud,²⁴ E. Latour,²⁴ M. Verderi,²⁴ P. J. Clark,²⁵ S. Playfer,²⁵ J. E. Watson,²⁵ M. Andreotti,^{26a,26b} D. Bettoni,^{26a} C. Bozzi,^{26a} R. Calabrese,^{26a,26b} A. Cecchi,^{26a,26b} G. Cibinetto,^{26a,26b} P. Franchini,^{26a,26b} E. Luppi,^{26a,26b} M. Negrini,^{26a,26b} A. Petrella,^{26a,26b} L. Piemontese,^{26a} V. Santoro,^{26a,26b} R. Baldini-Ferroli,²⁷ A. Calcaterra,²⁷ R. de Sangro,²⁷ G. Finocchiaro,²⁷ S. Pacetti,²⁷ P. Patteri,²⁷ I. M. Peruzzi,^{27,§} M. Piccolo,²⁷ M. Rama,²⁷ A. Zallo,²⁷ A. Buzzo,^{28a} R. Contri,^{28a,28b} M. Lo Vetere,^{28a,28b} M. M. Macri,^{28a} M. R. Monge,^{28a,28b} S. Passaggio,^{28a} C. Patrignani,^{28a,28b} E. Robutti,^{28a} A. Santroni,^{28a,28b} S. Tosi,^{28a,28b} K. S. Chaisanguanthum,²⁹ M. Morii,²⁹ A. Adametz,³⁰ J. Marks,³⁰ S. Schenk,³⁰ U. Uwer,³⁰ V. Klose,³¹ H. M. Lacker,³¹ D. J. Bard,³² P. D. Dauncey,³² J. A. Nash,³² M. Tibbetts,³² P. K. Behera,³³ X. Chai,³³ M. J. Charles,³³ U. Mallik,³³ J. Cochran,³⁴ H. B. Crawley,³⁴ L. Dong,³⁴ W. T. Meyer,³⁴ S. Prell,³⁴ E. I. Rosenberg,³⁴ A. E. Rubin,³⁴ Y. Y. Gao,³⁵ A. V. Gritsan,³⁵ Z. J. Guo,³⁵ C. K. Lae,³⁵ N. Arnaud,³⁶ J. Béquilleux,³⁶ A. D'Orazio,³⁶ M. Davier,³⁶ J. Firmino da Costa,³⁶ G. Grosdidier,³⁶ A. Höcker,³⁶ V. Lepeltier,³⁶ F. Le Diberder,³⁶ A. M. Lutz,³⁶ S. Pruvot,³⁶ P. Roudeau,³⁶ M. H. Schune,³⁶ J. Serrano,³⁶ V. Sordini,^{36,||} A. Stocchi,³⁶ G. Wormser,³⁶ D. J. Lange,³⁷ D. M. Wright,³⁷ I. Bingham,³⁸ J. P. Burke,³⁸ C. A. Chavez,³⁸ J. R. Fry,³⁸ E. Gabathuler,³⁸ R. Gamet,³⁸ D. E. Hutchcroft,³⁸ D. J. Payne,³⁸ C. Touramanis,³⁸ A. J. Bevan,³⁹ C. K. Clarke,³⁹ K. A. George,³⁹ F. Di Lodovico,³⁹ R. Sacco,³⁹ M. Sigamani,³⁹ G. Cowan,⁴⁰ H. U. Flaecher,⁴⁰ D. A. Hopkins,⁴⁰ S. Paramesvaran,⁴⁰ F. Salvatore,⁴⁰ A. C. Wren,⁴⁰ D. N. Brown,⁴¹ C. L. Davis,⁴¹ A. G. Denig,⁴² M. Fritsch,⁴² W. Gradl,⁴² G. Schott,⁴² K. E. Alwyn,⁴³ D. Bailey,⁴³ R. J. Barlow,⁴³ Y. M. Chia,⁴³ C. L. Edgar,⁴³ G. Jackson,⁴³ G. D. Lafferty,⁴³ T. J. West,⁴³ J. I. Yi,⁴³ J. Anderson,⁴⁴ C. Chen,⁴⁴ A. Jawahery,⁴⁴ D. A. Roberts,⁴⁴ G. Simi,⁴⁴ J. M. Tuggle,⁴⁴ C. Dallapiccola,⁴⁵ X. Li,⁴⁵ E. Salvati,⁴⁵ S. Saremi,⁴⁵ R. Cowan,⁴⁶ D. Dujmic,⁴⁶ P. H. Fisher,⁴⁶ G. Sciolla,⁴⁶ M. Spitznagel,⁴⁶ F. Taylor,⁴⁶ R. K. Yamamoto,⁴⁶ M. Zhao,⁴⁶ P. M. Patel,⁴⁷ S. H. Robertson,⁴⁷ A. Lazzaro,^{48a,48b} V. Lombardo,^{48a} F. Palombo,^{48a,48b} J. M. Bauer,⁴⁹ L. Cremaldi,⁴⁹ R. Godang,^{49,¶} R. Kroeger,⁴⁹ D. A. Sanders,⁴⁹ D. J. Summers,⁴⁹ H. W. Zhao,⁴⁹ M. Simard,⁵⁰ P. Taras,⁵⁰ F. B. Viaud,⁵⁰ H. Nicholson,⁵¹ G. De Nardo,^{52a,52b} L. Lista,^{52a} D. Monorchio,^{52a,52b} G. Onorato,^{52a,52b} C. Sciacca,^{52a,52b} G. Raven,⁵³ H. L. Snoek,⁵³ C. P. Jessop,⁵⁴ K. J. Knoepfel,⁵⁴ J. M. LoSecco,⁵⁴ W. F. Wang,⁵⁴ G. Benelli,⁵⁵ L. A. Corwin,⁵⁵ K. Honscheid,⁵⁵ H. Kagan,⁵⁵ R. Kass,⁵⁵ J. P. Morris,⁵⁵ A. M. Rahimi,⁵⁵ J. J. Regensburger,⁵⁵ S. J. Sekula,⁵⁵ Q. K. Wong,⁵⁵ N. L. Blount,⁵⁶ J. Brau,⁵⁶ R. Frey,⁵⁶ O. Igonkina,⁵⁶ J. A. Kolb,⁵⁶ M. Lu,⁵⁶ R. Rahmat,⁵⁶ N. B. Sinev,⁵⁶ D. Strom,⁵⁶ J. Strube,⁵⁶ E. Torrence,⁵⁶ G. Castelli,^{57a,57b} N. Gagliardi,^{57a,57b} M. Margoni,^{57a,57b} M. Morandin,^{57a} M. Posocco,^{57a} M. Rotondo,^{57a} F. Simonetto,^{57a,57b} R. Stroili,^{57a,57b} C. Voci,^{57a,57b} P. del Amo Sanchez,⁵⁸ E. Ben-Haim,⁵⁸ H. Briand,⁵⁸ G. Calderini,⁵⁸ J. Chauveau,⁵⁸ P. David,⁵⁸ L. Del Buono,⁵⁸ O. Hamon,⁵⁸ Ph. Leruste,⁵⁸ J. Ocariz,⁵⁸ A. Perez,⁵⁸ J. Prendki,⁵⁸ S. Sitt,⁵⁸ L. Gladney,⁵⁹ M. Biasini,^{60a,60b} R. Covarelli,^{60a,60b} E. Manoni,^{60a,60b} C. Angelini,^{61a,61b} G. Batignani,^{61a,61b} S. Bettarini,^{61a,61b} M. Carpinelli,^{61a,61b,**} A. Cervelli,^{61a,61b} F. Forti,^{61a,61b} M. A. Giorgi,^{61a,61b} A. Lusiani,^{61a,61c} G. Marchiori,^{61a,61b} M. Morganti,^{61a,61b} N. Neri,^{61a,61b} E. Paoloni,^{61a,61b} G. Rizzo,^{61a,61b} J. J. Walsh,^{61a} D. Lopes Pegna,⁶² C. Lu,⁶² J. Olsen,⁶² A. J. S. Smith,⁶² A. V. Telnov,⁶² F. Anulli,^{63a} E. Baracchini,^{63a,63b} G. Cavoto,^{63a} D. del Re,^{63a,63b} E. Di Marco,^{63a,63b} R. Faccini,^{63a,63b}

F. Ferrarotto,^{63a,63b} F. Ferroni,^{63a,63b} M. Gaspero,^{63a,63b} P.D. Jackson,^{63a} L. Li Gioi,^{63a} M. A. Mazzoni,^{63a} S. Morganti,^{63a} G. Piredda,^{63a} F. Polci,^{63a,63b} F. Renga,^{63a,63b} C. Voena,^{63a,63b} M. Ebert,⁶⁴ T. Hartmann,⁶⁴ H. Schröder,⁶⁴ R. Waldi,⁶⁴ T. Adye,⁶⁵ B. Franek,⁶⁵ E. O. Olaiya,⁶⁵ F. F. Wilson,⁶⁵ S. Emery,⁶⁶ M. Escalier,⁶⁶ L. Esteve,⁶⁶ S. F. Ganzhur,⁶⁶ G. Hamel de Monchenault,⁶⁶ W. Kozanecki,⁶⁶ G. Vasseur,⁶⁶ Ch. Yèche,⁶⁶ M. Zito,⁶⁶ X. R. Chen,⁶⁷ H. Liu,⁶⁷ W. Park,⁶⁷ M. V. Purohit,⁶⁷ R. M. White,⁶⁷ J. R. Wilson,⁶⁷ M. T. Allen,⁶⁸ D. Aston,⁶⁸ R. Bartoldus,⁶⁸ P. Bechtle,⁶⁸ J. F. Benitez,⁶⁸ R. Cenci,⁶⁸ J. P. Coleman,⁶⁸ M. R. Convery,⁶⁸ J. C. Dingfelder,⁶⁸ J. Dorfan,⁶⁸ G. P. Dubois-Felsmann,⁶⁸ W. Dunwoodie,⁶⁸ R. C. Field,⁶⁸ A. M. Gabareen,⁶⁸ S. J. Gowdy,⁶⁸ M. T. Graham,⁶⁸ P. Grenier,⁶⁸ C. Hast,⁶⁸ W. R. Innes,⁶⁸ J. Kaminski,⁶⁸ M. H. Kelsey,⁶⁸ H. Kim,⁶⁸ P. Kim,⁶⁸ M. L. Kocian,⁶⁸ D. W. G. S. Leith,⁶⁸ S. Li,⁶⁸ B. Lindquist,⁶⁸ S. Luitz,⁶⁸ V. Luth,⁶⁸ H. L. Lynch,⁶⁸ D. B. MacFarlane,⁶⁸ H. Marsiske,⁶⁸ R. Messner,⁶⁸ D. R. Muller,⁶⁸ H. Neal,⁶⁸ S. Nelson,⁶⁸ C. P. O'Grady,⁶⁸ I. Ofte,⁶⁸ A. Perazzo,⁶⁸ M. Perl,⁶⁸ B. N. Ratcliff,⁶⁸ A. Roodman,⁶⁸ A. A. Salnikov,⁶⁸ R. H. Schindler,⁶⁸ J. Schwiening,⁶⁸ A. Snyder,⁶⁸ D. Su,⁶⁸ M. K. Sullivan,⁶⁸ K. Suzuki,⁶⁸ S. K. Swain,⁶⁸ J. M. Thompson,⁶⁸ J. Va'vra,⁶⁸ A. P. Wagner,⁶⁸ M. Weaver,⁶⁸ C. A. West,⁶⁸ W. J. Wisniewski,⁶⁸ M. Wittgen,⁶⁸ D. H. Wright,⁶⁸ H. W. Wulsin,⁶⁸ A. K. Yarritu,⁶⁸ K. Yi,⁶⁸ C. C. Young,⁶⁸ V. Ziegler,⁶⁸ P. R. Burchat,⁶⁹ A. J. Edwards,⁶⁹ S. A. Majewski,⁶⁹ T. S. Miyashita,⁶⁹ B. A. Petersen,⁶⁹ L. Wilden,⁶⁹ S. Ahmed,⁷⁰ M. S. Alam,⁷⁰ J. A. Ernst,⁷⁰ B. Pan,⁷⁰ M. A. Saeed,⁷⁰ S. B. Zain,⁷⁰ S. M. Spanier,⁷¹ B. J. Wogland,⁷¹ R. Eckmann,⁷² J. L. Ritchie,⁷² A. M. Ruland,⁷² C. J. Schilling,⁷² R. F. Schwitters,⁷² B. W. Drummond,⁷³ J. M. Izen,⁷³ X. C. Lou,⁷³ F. Bianchi,^{74a,74b} D. Gamba,^{74a,74b} M. Pelliccioni,^{74a,74b} M. Bomben,^{75a,75b} L. Bosisio,^{75a,75b} C. Cartaro,^{75a,75b} G. Della Ricca,^{75a,75b} L. Lanceri,^{75a,75b} L. Vitale,^{75a,75b} V. Azzolini,⁷⁶ N. Lopez-March,⁷⁶ F. Martinez-Vidal,⁷⁶ D. A. Milanes,⁷⁶ A. Oyanguren,⁷⁶ J. Albert,⁷⁷ Sw. Banerjee,⁷⁷ B. Bhuyan,⁷⁷ H. H. F. Choi,⁷⁷ K. Hamano,⁷⁷ R. Kowalewski,⁷⁷ M. J. Lewczuk,⁷⁷ I. M. Nugent,⁷⁷ J. M. Roney,⁷⁷ R. J. Sobie,⁷⁷ T. J. Gershon,⁷⁸ P. F. Harrison,⁷⁸ J. Ilic,⁷⁸ T. E. Latham,⁷⁸ G. B. Mohanty,⁷⁸ H. R. Band,⁷⁹ X. Chen,⁷⁹ S. Dasu,⁷⁹ K. T. Flood,⁷⁹ Y. Pan,⁷⁹ M. Pierini,⁷⁹ R. Prepost,⁷⁹ C. O. Vuosalo,⁶⁸ and S. L. Wu⁷⁹

(BABAR Collaboration)

¹Laboratoire de Physique des Particules, IN2P3/CNRS et Université de Savoie, F-74941 Annecy-Le-Vieux, France

²Universitat de Barcelona, Facultat de Física, Departament ECM, E-08028 Barcelona, Spain

^{3a}INFN Sezione di Bari, I-70126 Bari, Italy

^{3b}Dipartimento di Fisica, Università di Bari, I-70126 Bari, Italy

⁴University of Bergen, Institute of Physics, N-5007 Bergen, Norway

⁵Lawrence Berkeley National Laboratory and University of California, Berkeley, California 94720, USA

⁶University of Birmingham, Birmingham, B15 2TT, United Kingdom

⁷Ruhr Universität Bochum, Institut für Experimentalphysik I, D-44780 Bochum, Germany

⁸University of Bristol, Bristol BS8 1TL, United Kingdom

⁹University of British Columbia, Vancouver, British Columbia, Canada V6T 1Z1

¹⁰Brunel University, Uxbridge, Middlesex UB8 3PH, United Kingdom

¹¹Budker Institute of Nuclear Physics, Novosibirsk 630090, Russia

¹²University of California at Irvine, Irvine, California 92697, USA

¹³University of California at Los Angeles, Los Angeles, California 90024, USA

¹⁴University of California at Riverside, Riverside, California 92521, USA

¹⁵University of California at San Diego, La Jolla, California 92093, USA

¹⁶University of California at Santa Barbara, Santa Barbara, California 93106, USA

¹⁷University of California at Santa Cruz, Institute for Particle Physics, Santa Cruz, California 95064, USA

¹⁸California Institute of Technology, Pasadena, California 91125, USA

¹⁹University of Cincinnati, Cincinnati, Ohio 45221, USA

²⁰University of Colorado, Boulder, Colorado 80309, USA

²¹Colorado State University, Fort Collins, Colorado 80523, USA

²²Technische Universität Dortmund, Fakultät Physik, D-44221 Dortmund, Germany

²³Technische Universität Dresden, Institut für Kern- und Teilchenphysik, D-01062 Dresden, Germany

²⁴Laboratoire Leprince-Ringuet, CNRS/IN2P3, Ecole Polytechnique, F-91128 Palaiseau, France

²⁵University of Edinburgh, Edinburgh EH9 3JZ, United Kingdom

^{26a}INFN Sezione di Ferrara, I-44100 Ferrara, Italy

^{26b}Dipartimento di Fisica, Università di Ferrara, I-44100 Ferrara, Italy

²⁷INFN Laboratori Nazionali di Frascati, I-00044 Frascati, Italy

^{28a}INFN Sezione di Genova, I-16146 Genova, Italy

^{28b}Dipartimento di Fisica, Università di Genova, I-16146 Genova, Italy

²⁹Harvard University, Cambridge, Massachusetts 02138, USA

- ³⁰Universität Heidelberg, Physikalisches Institut, Philosophenweg 12, D-69120 Heidelberg, Germany
- ³¹Humboldt-Universität zu Berlin, Institut für Physik, Newtonstr. 15, D-12489 Berlin, Germany
- ³²Imperial College London, London, SW7 2AZ, United Kingdom
- ³³University of Iowa, Iowa City, Iowa 52242, USA
- ³⁴Iowa State University, Ames, Iowa 50011-3160, USA
- ³⁵Johns Hopkins University, Baltimore, Maryland 21218, USA
- ³⁶Laboratoire de l'Accélérateur Linéaire, IN2P3/CNRS et Université Paris-Sud 11, Centre Scientifique d'Orsay, B. P. 34, F-91898 Orsay Cedex, France
- ³⁷Lawrence Livermore National Laboratory, Livermore, California 94550, USA
- ³⁸University of Liverpool, Liverpool L69 7ZE, United Kingdom
- ³⁹Queen Mary, University of London, London, E1 4NS, United Kingdom
- ⁴⁰University of London, Royal Holloway and Bedford New College, Egham, Surrey TW20 0EX, United Kingdom
- ⁴¹University of Louisville, Louisville, Kentucky 40292, USA
- ⁴²Johannes Gutenberg-Universität Mainz, Institut für Kernphysik, D-55099 Mainz, Germany
- ⁴³University of Manchester, Manchester M13 9PL, United Kingdom
- ⁴⁴University of Maryland, College Park, Maryland 20742, USA
- ⁴⁵University of Massachusetts, Amherst, Massachusetts 01003, USA
- ⁴⁶Massachusetts Institute of Technology, Laboratory for Nuclear Science, Cambridge, Massachusetts 02139, USA
- ⁴⁷McGill University, Montréal, Québec, Canada H3A 2T8
- ^{48a}INFN Sezione di Milano, I-20133 Milano, Italy
- ^{48b}Dipartimento di Fisica, Università di Milano, I-20133 Milano, Italy
- ⁴⁹University of Mississippi, University, Mississippi 38677, USA
- ⁵⁰Université de Montréal, Physique des Particules, Montréal, Québec, Canada H3C 3J7
- ⁵¹Mount Holyoke College, South Hadley, Massachusetts 01075, USA
- ^{52a}INFN Sezione di Napoli, I-80126 Napoli, Italy
- ^{52b}Dipartimento di Scienze Fisiche, Università di Napoli Federico II, I-80126 Napoli, Italy
- ⁵³NIKHEF, National Institute for Nuclear Physics and High Energy Physics, NL-1009 DB Amsterdam, The Netherlands
- ⁵⁴University of Notre Dame, Notre Dame, Indiana 46556, USA
- ⁵⁵Ohio State University, Columbus, Ohio 43210, USA
- ⁵⁶University of Oregon, Eugene, Oregon 97403, USA
- ^{57a}INFN Sezione di Padova, I-35131 Padova, Italy
- ^{57b}Dipartimento di Fisica, Università di Padova, I-35131 Padova, Italy
- ⁵⁸Laboratoire de Physique Nucléaire et de Hautes Energies, IN2P3/CNRS, Université Pierre et Marie Curie-Paris6, Université Denis Diderot-Paris7, F-75252 Paris, France
- ⁵⁹University of Pennsylvania, Philadelphia, Pennsylvania 19104, USA
- ^{60a}INFN Sezione di Perugia, I-06100 Perugia, Italy
- ^{60b}Dipartimento di Fisica, Università di Perugia, I-06100 Perugia, Italy
- ^{61a}INFN Sezione di Pisa, I-56127 Pisa, Italy
- ^{61b}Dipartimento di Fisica, Università di Pisa, I-56127 Pisa, Italy
- ^{61c}Scuola Normale Superiore di Pisa, I-56127 Pisa, Italy
- ⁶²Princeton University, Princeton, New Jersey 08544, USA
- ^{63a}INFN Sezione di Roma, I-00185 Roma, Italy
- ^{63b}Dipartimento di Fisica, Università di Roma La Sapienza, I-00185 Roma, Italy
- ⁶⁴Universität Rostock, D-18051 Rostock, Germany
- ⁶⁵Rutherford Appleton Laboratory, Chilton, Didcot, Oxon, OX11 0QX, United Kingdom
- ⁶⁶CEA, Irfu, SPP, Centre de Saclay, F-91191 Gif-sur-Yvette, France
- ⁶⁷University of South Carolina, Columbia, South Carolina 29208, USA
- ⁶⁸Stanford Linear Accelerator Center, Stanford, California 94309, USA
- ⁶⁹Stanford University, Stanford, California 94305-4060, USA
- ⁷⁰State University of New York, Albany, New York 12222, USA
- ⁷¹University of Tennessee, Knoxville, Tennessee 37996, USA
- ⁷²University of Texas at Austin, Austin, Texas 78712, USA
- ⁷³University of Texas at Dallas, Richardson, Texas 75083, USA
- ^{74a}INFN Sezione di Torino, I-10125 Torino, Italy
- ^{74b}Dipartimento di Fisica Sperimentale, Università di Torino, I-10125 Torino, Italy
- ^{75a}INFN Sezione di Trieste, I-34127 Trieste, Italy
- ^{75b}Dipartimento di Fisica, Università di Trieste, I-34127 Trieste, Italy
- ⁷⁶IFIC, Universitat de Valencia-CSIC, E-46071 Valencia, Spain
- ⁷⁷University of Victoria, Victoria, British Columbia, Canada V8W 3P6
- ⁷⁸Department of Physics, University of Warwick, Coventry CV4 7AL, United Kingdom
- ⁷⁹University of Wisconsin, Madison, Wisconsin 53706, USA

(Received 1 August 2008; published 23 April 2009)

Using a sample of $383 \times 10^6 B\bar{B}$ events collected by the *BABAR* experiment, we measure sums of seven exclusive final states $B \rightarrow X_{d(s)}\gamma$, where $X_d(X_s)$ is a nonstrange (strange) charmless hadronic system in the mass range 0.6–1.8 GeV/ c^2 . After correcting for unmeasured decay modes in this mass range, we obtain a branching fraction for $b \rightarrow d\gamma$ of $(7.2 \pm 2.7(\text{stat}) \pm 2.3(\text{syst})) \times 10^{-6}$. Taking the ratio of X_d to X_s we find $\Gamma(b \rightarrow d\gamma)/\Gamma(b \rightarrow s\gamma) = 0.033 \pm 0.013(\text{stat}) \pm 0.009(\text{syst})$, from which we determine $|V_{td}/V_{ts}| = 0.177 \pm 0.043$.

DOI: 10.1103/PhysRevLett.102.161803

PACS numbers: 13.20.He, 12.15.Hh

The decays $b \rightarrow d\gamma$ and $b \rightarrow s\gamma$ are flavor-changing neutral current processes. They are forbidden at tree level in the standard model (SM), but can occur via one-loop electroweak penguin diagrams involving the top quark. In the SM, the inclusive rate for $b \rightarrow d\gamma$ is suppressed compared to $b \rightarrow s\gamma$ by $|V_{td}/V_{ts}|^2$, where V_{td} and V_{ts} are Cabibbo-Kobayashi-Maskawa matrix elements. Measurements of $|V_{td}/V_{ts}|$ from $B \rightarrow (\rho, \omega)\gamma$ and $B \rightarrow K^*\gamma$ [1] have theoretical uncertainties of 7% from weak annihilation and hadronic form factors [2]. A measurement of the inclusive decay $b \rightarrow d\gamma$ relative to $b \rightarrow s\gamma$ could determine $|V_{td}/V_{ts}|$ with reduced theoretical uncertainties compared to the exclusive modes [3]. In theories beyond the SM [4], new particles may appear differently in the penguin loop diagrams for $b \rightarrow d\gamma$ and $b \rightarrow s\gamma$ compared to the box diagrams responsible for B_d and B_s mixing [5], leading to differences in $|V_{td}/V_{ts}|$.

This Letter presents the first measurement of $|V_{td}/V_{ts}|$ from $b \rightarrow d\gamma$ and $b \rightarrow s\gamma$ inclusive decays including the region above the ρ/ω resonances, with systematic uncertainties largely independent of those from the measurement provided by the exclusive reconstruction of the $B \rightarrow (\rho, \omega)\gamma$ and $B \rightarrow K^*\gamma$ decay channels.

We present measurements of the rare decays $B \rightarrow X_d\gamma$ using seven exclusive final states $B^0 \rightarrow \pi^+\pi^-\gamma$, $B^+ \rightarrow \pi^+\pi^0\gamma$, $B^+ \rightarrow \pi^+\pi^-\pi^+\gamma$, $B^0 \rightarrow \pi^+\pi^-\pi^0\gamma$, $B^0 \rightarrow \pi^+\pi^-\pi^+\pi^-\gamma$, $B^+ \rightarrow \pi^+\pi^-\pi^+\pi^0\gamma$ and $B^+ \rightarrow \pi^+\eta\gamma$ [6], in the hadronic mass range 0.6–1.0 GeV/ c^2 (which contains the ρ and ω resonances), and in the previously unmeasured region 1.0–1.8 GeV/ c^2 . We combine the results and correct for decay modes that are not reconstructed to obtain the inclusive branching fraction for $b \rightarrow d\gamma$ in the mass range 0.6–1.8 GeV/ c^2 . A parallel analysis of $B \rightarrow X_s\gamma$ using these modes with a K^+ replacing the first π^+ allows us to measure the ratio of inclusive rates $\Gamma(b \rightarrow d\gamma)/\Gamma(b \rightarrow s\gamma)$ in the same mass range.

This analysis uses $383 \times 10^6 B\bar{B}$ pairs collected at the $Y(4S)$ resonance with the *BABAR* detector [7] at the PEP-II B factory. The high-energy γ is defined as an isolated energy cluster in the CsI(Tl) calorimeter, with a shape consistent with a single γ , and energy $1.15 < E_\gamma^* < 3.5$ GeV in the center-of-mass (c.m.) frame. We remove γ s forming a π^0 (η) candidate with another γ of energy greater than 30(250) MeV, if the two-photon invariant mass is in the range $105 < m_{\gamma\gamma} < 155$ MeV/ c^2 ($500 < m_{\gamma\gamma} < 590$ MeV/ c^2).

Charged particle tracks are reconstructed by means of a 5-layer silicon vertex detector and a 40-layer drift chamber coaxial with a 1.5 T magnetic field; a minimum laboratory momentum of 300 MeV/ c is required. To distinguish π^+ s from K^+ s we combine information from the detector of internally reflected Cherenkov light with specific ionisation energy loss measured in the tracking system. At a typical π^+ energy of 1 GeV, π^+ selection efficiency is 85% with K^+ misidentification rate 3%. K^+ s are selected by inverting the pion selection criteria. We reconstruct a $\pi^0(\eta)$ candidate with laboratory momentum greater than 300 MeV/ c from a pair of γ s, each with energy >20 MeV and satisfying $107 < m_{\gamma\gamma} < 145$ MeV/ c^2 ($470 < m_{\gamma\gamma} < 620$ MeV/ c^2). The $\pi^0(\eta)$ candidate, the high-energy γ and the selected charged tracks are combined to form a B meson candidate consistent with one of the decay modes. For a $B \rightarrow X_s\gamma$ decay one K^+ is required, with all other tracks required to be π^+ s. For $B \rightarrow X_d\gamma$ decays, all tracks are required to be identified as π^+ s. The charged particles are combined to form a common vertex for which the vertex fit probability is required to be greater than 2%.

The backgrounds encountered in this analysis arise mostly from continuum $e^+e^- \rightarrow q\bar{q}$ events, $q = (u, d, s, c)$, in which an energetic γ comes from either initial state radiation or the decay of a $\pi^0(\eta)$. We require $R_2 < 0.9$ and $|\cos\theta_T| < 0.8$, where R_2 is the ratio of the 2nd to 0th Fox-Wolfgram moments [8], and θ_T is the angle between the γ and the thrust axis of the rest of the event (ROE) in the c.m. frame. The ROE includes all the charged tracks and neutral energy in the calorimeter, excluding the B candidate.

The quantity $\cos\theta_T$ and 12 other variables that distinguish signal from continuum events are combined in a neural network (NN). These include the ratio R_2' , which is R_2 calculated in the frame recoiling against the γ momentum, the B meson production angle θ_B^* in the c.m. frame with respect to the beam axis, and five Legendre polynomial moments of the ROE with respect to both the thrust axis of the ROE and the direction of the high-energy γ . Differences in lepton and kaon production between background and B decays are exploited by including five flavor-tagging variables applied to the ROE [9]. We optimize the NN configuration for maximal discrimination between signal and background; this gives 50% signal efficiency and 0.5% misidentification of continuum, based on a Monte Carlo (MC) simulation.

We use the kinematic variables $\Delta E = E_B^* - E_{\text{beam}}^*$ and $m_{\text{ES}} = \sqrt{E_{\text{beam}}^{*2} - |\vec{p}_B^*|^2}$, where E_B^* and \vec{p}_B^* are the c.m. energy and momentum of the B candidate, and E_{beam}^* is the c.m. beam energy. Signal events should have a ΔE distribution centered at zero with a resolution ~ 30 MeV, and an m_{ES} distribution centered at the B meson mass with a resolution ~ 3 MeV/ c^2 . We retain candidates with $-0.3 \text{ GeV} < \Delta E < 0.2 \text{ GeV}$ and $m_{\text{ES}} > 5.22 \text{ GeV}/c^2$ to allow the combinatorial background yield to be extracted from a fit to the data. After all selection criteria are applied there are, on average, 1.75 candidates per event. In events with multiple candidates we select the one with the best $\pi^0(\eta)$ mass, or, where there is no $\pi^0(\eta)$, we select the candidate with the best vertex fit probability.

The signal yield in each B decay category is determined from a two-dimensional unbinned maximum likelihood fit to the $(\Delta E, m_{\text{ES}})$ distributions of the sums of all seven final states. We consider the following contributions: signal, combinatorial backgrounds from continuum processes, $B \rightarrow X\pi^0/\eta$ decays, backgrounds from other B decays, and cross-feed from misreconstructed signal $B \rightarrow X\gamma$ decays. The fit to the $B \rightarrow X_d\gamma$ sample contains a component from misidentified $B \rightarrow X_s\gamma$ decays, but we neglect the small $B \rightarrow X_d\gamma$ background in the $B \rightarrow X_s\gamma$ sample. The B background yields are determined from MC simulation, whereas the continuum background yield is free to vary in the fit.

Each background contribution is modeled by a probability density function (PDF) determined from MC events. Each signal PDF is the product of one-dimensional m_{ES} and ΔE distributions determined from fits to the $B \rightarrow K^*\gamma$ data. For the signal cross-feed component, and the $B \rightarrow X_s\gamma$ background in the $B \rightarrow X_d\gamma$ fit, MC studies indicate that two-dimensional histogram PDFs are required to account for correlations that are not present in signal MC events. The contributions from $B \rightarrow X\pi^0/\eta$ are modeled by a Gaussian peak in each of ΔE and m_{ES} , where ΔE is displaced by -80 MeV due to the missing photon. The $B \rightarrow X_s\gamma$ background in the $B \rightarrow X_d\gamma$ sample also peaks, with ΔE displaced by -50 MeV due to K^+ misidentification. Continuum and other nonpeaking backgrounds are described by an ARGUS shape [10] in m_{ES} and a second-order polynomial in ΔE .

We perform separate fits for $B \rightarrow X_d\gamma$ and $B \rightarrow X_s\gamma$, in the two hadronic mass ranges. The signal and continuum yields, the continuum ARGUS shape parameter and the continuum polynomial shape parameters are allowed to vary. We scale the cross-feed contribution proportionally to the fitted signal yield, refit, and iterate until the fit converges. The fit projections for $B \rightarrow X_s\gamma$ and $B \rightarrow X_d\gamma$ are shown in Fig. 1.

The fit results are summarized in Table I. The reconstruction efficiency depends on the distribution of the signal yield among the final states. For X_s we obtain this distribution from the data, but for X_d this is not possible

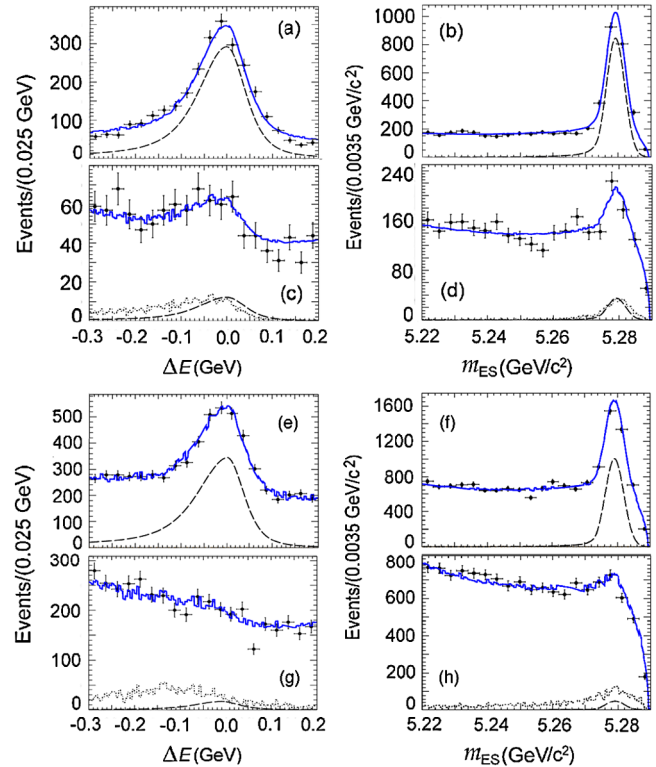


FIG. 1 (color online). Projections of the fits to data in the hadronic mass range $0.6\text{--}1.0 \text{ GeV}/c^2$ (a)–(d) and $1.0\text{--}1.8 \text{ GeV}/c^2$ (e)–(h). Projections of ΔE with $5.275 < m_{\text{ES}} < 5.286 \text{ GeV}/c^2$ for (a),(e) $B \rightarrow X_s\gamma$ and (c),(f) $B \rightarrow X_d\gamma$, and of m_{ES} with $-0.1 < \Delta E < 0.05 \text{ GeV}$ for (b),(g) $B \rightarrow X_s\gamma$ and (d), (h) $B \rightarrow X_d\gamma$. Data (points) are compared with the sum of all the fit contributions (solid curve) including the signal (dashed curve) and the $B \rightarrow X_s\gamma$ contribution in the $B \rightarrow X_d\gamma$ fit (dotted curve).

and so we use the phase space fragmentation model implemented in JETSET [11] for this purpose.

The branching fractions in Table II are obtained after correcting for missing final states. In the low mass region for both channels we assume that there are no nonresonant decays, an assumption consistent with our data in the $B \rightarrow X_s\gamma$ channel. Our low mass $B \rightarrow X_s\gamma$ measurement agrees with previous rate measurements for $B \rightarrow K^*\gamma$ [12], after accounting for the 50% of decays to neutral kaons. For the X_d modes at low mass, the fraction of nonreconstructed ρ and ω decays is small, and we find a branching fraction of

TABLE I. Signal yield (N_S), average efficiency (ϵ) and partial branching fraction (\mathcal{B}) for the measured decay modes. The first error is statistical, the second systematic.

$M(X)[\text{GeV}/c^2]$	N_S	ϵ	$\mathcal{B}(\times 10^{-6})$
$0.6 < M(X_s) < 1.0$	1543 ± 46	8.5%	$23.7 \pm 0.7 \pm 1.7$
$0.6 < M(X_d) < 1.0$	66 ± 26	7.0%	$1.2 \pm 0.5 \pm 0.1$
$1.0 < M(X_s) < 1.8$	2279 ± 75	6.1%	$48.7 \pm 1.6 \pm 4.1$
$1.0 < M(X_d) < 1.8$	107 ± 47	5.2%	$2.7 \pm 1.2 \pm 0.4$

TABLE II. Branching fractions $\mathcal{B}(\times 10^{-6})$ and their ratio in the two mass regions of $M(X) \times [\text{GeV}/c^2]$, after correcting for missing final states. The first error is statistical and the second systematic.

$M(X)$	$\mathcal{B}(b \rightarrow d\gamma)$	$\mathcal{B}(b \rightarrow s\gamma)$	$\mathcal{B}(b \rightarrow d\gamma)/\mathcal{B}(b \rightarrow s\gamma)$
0.6–1.0	$1.2 \pm 0.5 \pm 0.1$	$47 \pm 1 \pm 3$	$0.026 \pm 0.011 \pm 0.002$
1.0–1.8	$6.0 \pm 2.6 \pm 2.3$	$168 \pm 14 \pm 33$	$0.036 \pm 0.015 \pm 0.009$
0.6–1.8	$7.2 \pm 2.7 \pm 2.3$	$215 \pm 14 \pm 33$	$0.033 \pm 0.013 \pm 0.009$

$(1.2 \pm 0.5) \times 10^{-6}$, in agreement with previous measurements of $\mathcal{B}(B \rightarrow (\rho, \omega)\gamma)$ [1]. In the high mass region for both channels, we correct for missing final states with ≥ 5 stable particles, or with multiple π^0 s, by using the fragmentation model described above. Alternative fragmentation models are used to estimate the associated uncertainty, as described below.

The sources of systematic uncertainty in the measurement of the branching fractions are listed in Table III. These include uncertainty in track reconstruction efficiency, γ and π^0/η reconstruction, the π^0/η veto, the NN selection, and the number of $B\bar{B}$ pairs. The 2% uncertainty in K^+/π^+ particle identification and the 20% uncertainty in K^+ misidentification, which affects the fixed $B \rightarrow X_s\gamma$ contribution to the $B \rightarrow X_d\gamma$ fits, do not cancel in the ratio. The systematic errors associated with the variation of the fit PDFs also do not cancel because of the very different signal to background ratios in the two samples. We vary the signal PDF parameters within the range allowed by the fit to the $B \rightarrow K^*\gamma$ data. The normalization of the signal cross-feed is varied by $\pm 30\%$, and the contribution of $B \rightarrow X\pi^0/\eta$ by $\pm 100\%$, in accordance with MC studies. The remaining peaking B backgrounds, including the $B \rightarrow X_s\gamma$ contribution to the $B \rightarrow X_d\gamma$ fits, are varied by $\pm 20\%$. We use simulated signal and background event samples to assign a systematic uncertainty due to possible bias in the fit method.

There is an additional systematic error on the efficiency due to the uncertainties in the measured fragmentation of the X_s hadronic system into the seven $B \rightarrow X_s\gamma$ final states. The equivalent error for $B \rightarrow X_d\gamma$ is obtained by comparing our fragmentation model for $B \rightarrow X_d\gamma$ to the fragmentation observed for $B \rightarrow X_s\gamma$ data. We assume that these errors are independent and so do not cancel in the ratio of branching fractions.

Table III also shows the systematic errors associated with corrections for the missing final states. There is no information from the data on the missing fraction of high multiplicity final states with ≥ 5 stable hadrons, or on the missing fraction of other final states with ≥ 1 π^0 or η mesons. We vary these fractions by $\pm 50\%$ relative to their default phase space fragmentation values. Our choice of a $\pm 50\%$ variation is motivated by studies of alternative MC signal models in which we replace half of the nonresonant width in the 1.0–1.8 GeV/ c^2 mass range with a mix of X_d

or X_s resonances. The missing fraction errors partially cancel in the ratio when the $\pm 50\%$ variations are made in the same direction for $b \rightarrow d\gamma$ and $b \rightarrow s\gamma$.

We take the spectral shape of the high-energy γ from Ref. [13] using the values $(m_b, \mu_\pi^2) = (4.65 \text{ GeV}/c^2, -0.52 \text{ GeV}^2)$ extracted from fits to $b \rightarrow s\gamma$ and $b \rightarrow c\ell\nu$ data [14]. We vary these shape parameters in a correlated way between $(m_b, \mu_\pi^2) = (4.60 \text{ GeV}/c^2, -0.60 \text{ GeV}^2)$ and $(m_b, \mu_\pi^2) = (4.70 \text{ GeV}/c^2, -0.45 \text{ GeV}^2)$. Systematic errors on the branching fractions result from these variations, but they are small and cancel in the ratio. The fraction of the spectrum in the mass range 0.6–1.8 GeV/ c^2 is estimated to be $(51 \pm 4)\%$ for $b \rightarrow d\gamma$ and $(50 \pm 4)\%$ for $b \rightarrow s\gamma$. We do not extrapolate the ratio of branching fractions to $M_X > 1.8 \text{ GeV}/c^2$, and so these errors, which mostly cancel in the ratio, are not included in Table III. If we make this correction, we obtain $\mathcal{B}(b \rightarrow d\gamma) = (1.4 \pm 0.5 \pm 0.4 \pm 0.1) \times 10^{-5}$ and $\mathcal{B}(b \rightarrow s\gamma) = (4.3 \pm 0.3 \pm 0.7 \pm 0.2) \times 10^{-4}$, where the first error is statistical, the second systematic and the third accounts for the uncertainty in extrapolating to the mass

TABLE III. Systematic errors on the measured partial and total branching fractions \mathcal{B} . The final column shows systematic errors that do not cancel in the ratio of rates.

Systematic Error Source	$M(X_s)$		$M(X_d)$		X_d/X_s Ratio
	0.6–1.0	1.0–1.8	0.6–1.0	1.0–1.8	
Tracking	1.7%	1.7%	1.7%	1.7%	
High-energy photon	2.5%	2.5%	2.5%	2.5%	
π^0/η reconstruction	1.7%	1.7%	1.7%	1.7%	
π^0/η veto	1.0%	1.0%	1.0%	1.0%	
K/π identification	2.0%	2.0%	2.0%	2.0%	2.0%
Neural network	5.0%	5.0%	5.0%	5.0%	
$B\bar{B}$ pair counting	1.1%	1.1%	1.1%	1.1%	
Fit PDFs	2.4%	3.6%	7.0%	8.3%	8.7%
Backgrounds	0.3%	0.4%	2.4%	6.1%	5.4%
Fit bias	0.4%	1.7%	0.4%	3.3%	3.0%
Fragmentation		3.6%		7.7%	8.5%
Partial \mathcal{B}	7.0%	11.4%	10.0%	14.8%	13.8%
Missing ≥ 5 body		5.6%		25.8%	21.0%
Other missing states		17.0%		23.8%	7.1%
Spectrum Model		1.8%		1.6%	
Total \mathcal{B}	7.0%	21.2%	10.0%	38.1%	26.1%

range. The result for $B \rightarrow X_s \gamma$ is consistent with the measured inclusive $b \rightarrow s \gamma$ branching fraction of $(3.55 \pm 0.24) \times 10^{-4}$ [12].

We convert the ratio of partial widths from the full mass range $0.6\text{--}1.8 \text{ GeV}/c^2$, $\Gamma(b \rightarrow d_s \gamma)/\Gamma(b \rightarrow s \gamma) = 0.033 \pm 0.013 \pm 0.009$, into a value for $|V_{td}/V_{ts}|$ using Table I and Eq. (26) of Ref. [3]. We obtain $|V_{td}/V_{ts}| = 0.177 \pm 0.043 \pm 0.001$, where the first error is experimental, including systematic errors, and the second error is from theory. The theory error includes uncertainties in the CKM parameters $\bar{\rho}$ and $\bar{\eta}$, and on $1/m_c^2$ and $1/m_b^2$ corrections, but includes no uncertainty for the restriction to the region below $1.8 \text{ GeV}/c^2$.

As a check, we use the low mass region to determine $|V_{td}/V_{ts}|$ using predictions for exclusive $B \rightarrow (\rho, \omega) \gamma$ and $B \rightarrow K^* \gamma$ from [2]. We find $|V_{td}/V_{ts}| = 0.214 \pm 0.046 \pm 0.028$ where the errors are as before. This is in good agreement with previously published results [1].

In summary, we have made the first measurement of $B \rightarrow X_d \gamma$ decays in the hadronic mass range up to $1.8 \text{ GeV}/c^2$, and have extracted $|V_{td}/V_{ts}|$ from an inclusive model with small theoretical uncertainties. These results are consistent with the measurements of $|V_{td}/V_{ts}|$ from the exclusive decays $B \rightarrow (\rho, \omega) \gamma$ [1], and with B_s/B_d oscillations [5]. Future studies applying this method to larger data sets could provide a substantial improvement in the determination of this quantity via radiative B meson decays. This offers the possibility that new physics effects could be revealed by the comparison of this determination with that from B_d/B_s oscillations. A measurement of the CP -violating parameters for inclusive $b \rightarrow d \gamma$ may also be possible.

We are grateful for the excellent luminosity and machine conditions provided by our PEP-II colleagues, and for the substantial dedicated effort from the computing organizations that support *BABAR*. The collaborating institutions wish to thank SLAC for its support and kind hospitality. This work is supported by DOE and NSF (USA), NSERC (Canada), CEA and CNRS-IN2P3 (France), BMBF and DFG (Germany), INFN (Italy), FOM (The Netherlands), NFR (Norway), MES (Russia), MEC (Spain), and STFC (United Kingdom). Individuals have received support from

the Marie Curie EIF (European Union) and the A. P. Sloan Foundation.

*Deceased.

†Now at Temple University, Philadelphia, PA 19122, USA.

‡Now at Tel Aviv University, Tel Aviv, 69978, Israel.

§Also with Università di Perugia, Dipartimento di Fisica, Perugia, Italy.

||Also with Università di Roma La Sapienza, I-00185 Roma, Italy.

¶Now at University of South Alabama, Mobile, AL 36688, USA.

**Also with Università di Sassari, Sassari, Italy.

- [1] B. Aubert *et al.* (*BABAR* Collaboration), *Phys. Rev. Lett.* **98**, 151802 (2007); D. Mohapatra *et al.* (*Belle* Collaboration), *Phys. Rev. Lett.* **96**, 221601 (2006).
- [2] P. Ball, G. Jones, and R. Zwicky, *Phys. Rev. D* **75**, 054004 (2007).
- [3] A. Ali, H. Asatrian, and C. Greub, *Phys. Lett. B* **429**, 87 (1998).
- [4] S. Bertolini, F. Borzumati, and A. Masiero, *Nucl. Phys. B* **294**, 321 (1987); H. Baer and M. Brhlik, *Phys. Rev. D* **55**, 3201 (1997); J. Hewett and J. Wells, *Phys. Rev. D* **55**, 5549 (1997); M. Carena *et al.*, *Phys. Lett. B* **499**, 141 (2001).
- [5] W.-M. Yao *et al.* (Particle Data Group), *J. Phys. G* **33**, 1 (2006).
- [6] Charge conjugate states are implied throughout this paper.
- [7] B. Aubert *et al.* (*BABAR* Collaboration), *Nucl. Instrum. Methods Phys. Res., Sect. A* **479**, 1 (2002).
- [8] G. C. Fox and S. Wolfram, *Nucl. Phys.* **B149**, 413 (1979).
- [9] B. Aubert *et al.* (*BABAR* Collaboration), *Phys. Rev. Lett.* **89**, 201802 (2002).
- [10] The ARGUS function is defined as: $P(x) = x[1 - (\frac{x}{m})^2]^p \exp(c[1 - (\frac{x}{m})^2])$, H. Albrecht *et al.* (ARGUS Collaboration), *Phys. Lett. B* **185**, 218 (1987).
- [11] T. Sjostrand, arXiv:hep-ph/9508391; T. Sjostrand, *Comput. Phys. Commun.* **82**, 74 (1994).
- [12] E. Barberio *et al.* (Heavy Flavor Averaging Group), arXiv:0704.3575.
- [13] A.L. Kagan and M. Neubert, *Phys. Rev. D* **58**, 094012 (1998).
- [14] O. Buchmüller and H. Flächer, *Phys. Rev. D* **73**, 073008 (2006).